Characterization of Electromagnetic Field-Transmission Line Coupling of Radiated Emission and Immunity Using TEM Cell Measurement

Chunlei Shi[1, *], Changchun Chai[1], Yintang Yang[1], Zhenyang Ma[1], Liping Qiao[2], and Xinhai Yu[1]

Abstract—An analytic model is proposed to estimate the electromagnetic field transmission line coupling for both radiated emission and immunity using TEM cell measurements. Further, a coupling impedance is introduced to determine the domination between electric and magnetic fields of the field-line coupling. Comparison of measurement and calculation results confirms the accuracy of the model. The model and coupling impedance can be helpful for the suppression of radiated emission and the enhancement of radiated immunity of transmission lines in electromagnetic compatibility design of electronic systems.

1. INTRODUCTION

Radiated emission and radiated immunity are two essential parts of electromagnetic compatibility (EMC) of electronic devices. Electronic devices commonly consist of one or more printed circuit boards (PCBs). PCBs contain components and traces. Traces are one of the key paths to transfer radiated electromagnetic interference (EMI) in to or out of electronic systems via electric and magnetic fields. Therefore, characterizations of couplings between EM field and traces become critical for EMC design and analysis.

In recent years, intensive efforts have been made on line-to-field and field-to-line couplings by using a transverse electromagnetic (TEM) or gigahertz TEM (GTEM) cell [1–11]. The TEM/GTEM cell measurement is specified by several international standards IEC 61967-2 [12] and IEC 62132-2 [13] for radiated emission and immunity tests. Mutual capacitance and mutual inductance were introduced to represent electric and magnetic field couplings of field-line coupling investigations [1–11] respectively. These components were applied for estimating radiated emission and immunity predictions.

Analytic circuit models in [9] and [11] by the authors used the termination effect to obtain mutual capacitance and inductance for frequency-domain radiated emission and time-domain radiated immunity estimations, respectively. Based on the previous works, we propose a modified analytic circuit model for both radiated emission and immunity predictions in frequency domain. Then, a coupling impedance is introduced to describe the coupling feature of a TEM cell and a microstrip line. Measurement and calculation results confirm the availability of the analytic model.

This paper is organized as follows. The analytic model is presented in Section 2. Measurement setup and results are described and discussed in Section 3. Conclusions are drawn in Section 4.

2. AN ANALYTIC MODEL OF FIELD-LINE COUPLING

Mutual capacitance C_{TEM} and mutual inductance M_{TEM} are adopted to represent the electric and magnetic field couplings between a TEM cell and a microstrip line, as shown in Fig. 1. The TEM cell approximates a 50-Ω transmission line and the TEM mode inside propagates along the length direction of the cell. Therefore, the microstrip line under test is placed parallel to the length direction of the TEM cell in order to get both electric and magnetic field couplings at the same time.
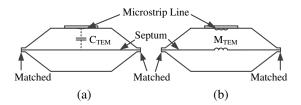

Figure 1. Mutual capacitance and mutual inductance for electric (a) and magnetic (b) field couplings of a TEM cell and a microstrip line.

2.1. Line-to-Field Coupling Model

The analytic model of line-to-field coupling in [4] treated the inductions on the septum of a TEM cell as individual current and voltage sources. The voltage V_{MS} and current I_{MS} at the distance z from the load along the microstrip line are functions of position z ($z \leq l$, l is the length of the microstrip line), and can be expressed in terms of the reflection coefficient Γ_0 [14]:

$$V_{\text{MS}}^{\text{RE}}(z) = V_{\text{in}}(e^{j\beta z} + \Gamma_0 e^{-j\beta z}) \tag{1}$$

$$I_{\text{MS}}^{\text{RE}}(z) = \frac{V_{\text{in}}}{Z_0}(e^{j\beta z} - \Gamma_0 e^{-j\beta z}) \tag{2}$$

where V_{in} is the voltage amplitude of an EMI injected into the microstrip line; $\beta = 2\pi/\lambda_{\text{e}}$ is the phase constant; λ_{e} is the wavelength propagating in the microstrip line; $\Gamma_0 = (Z_{\text{L}} - Z_0)/(Z_{\text{L}} + Z_0)$ is the reflection coefficient, in which Z_0 and Z_{L} are the characteristic impedance and the load impedance of the microstrip line, respectively.

According to the coupling mechanism of the TEM cell measurement, it can be assumed that the measured voltage at the tapered end of the TEM cell is contributed to the couplings between the septum and the small enough divided parts of the microstrip line. It means that the coupling can decrease to zero at certain high frequencies due to the fluctuations of $V_{\text{MS}}(z)$ and $I_{\text{MS}}(z)$. The length l of microstrip lines we considered is much shorter than λ_{e} (l less than $\lambda_{\text{e}}/10$). Therefore, the contributions of the whole line can be considered as a normalized voltage and current as follows

$$V_{\text{MS}}^{\text{RE}} = \frac{\int_0^l |V_{\text{MS}}^{\text{RE}}(z)|dz}{\int_0^l dz} \tag{3}$$

$$I_{\text{MS}}^{\text{RE}} = \frac{\int_0^l |I_{\text{MS}}^{\text{RE}}(z)|dz}{\int_0^l dz}. \tag{4}$$

Then, the induced voltage of the septum can be derived from equivalent circuits of a microstrip line to electric and magnetic field couplings for radiated emission in Fig. 2

$$V_{\text{septum}} = \frac{1}{2}\left(V_{\text{EC}}^{\text{RE}} \pm V_{\text{MC}}^{\text{RE}}\right) = \frac{1}{2}\omega\left(C_{\text{TEM}}Z_{\text{TEM}}V_{\text{MS}}^{\text{RE}} \pm M_{\text{TEM}}I_{\text{MS}}^{\text{RE}}\right) \tag{5}$$

where $\omega = 2\pi f$ is the angular frequency of the EMI in a form of continuous wave and $Z_{\text{TEM}} = 50\,\Omega$ the characteristic impedance of the TEM cell.
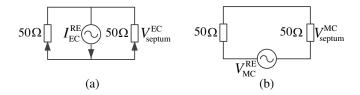
Figure 2. Equivalent circuits of a microstrip line to electric and magnetic field couplings for radiated emission: (a) electric field coupling, (b) magnetic field coupling.

2.2. Field-to-Line Coupling Model

When an EMI signal is injected into a TEM cell, the alternating voltage and current of the EMI generate electric field and magnetic field inside the TEM cell, respectively. The generated electric field induces a common mode current along the microstrip line, whereas the magnetic field induces a differential mode voltage along the line. The voltages induced by electric field coupling are in phase at both ends of a line, while those induced by magnetic field coupling are out of phase. The inductions along the line by electric and magnetic field-to-line couplings can be treated as voltage and current sources. These sources depend on the alternating frequency of the EMI and can be expressed in terms of mutual capacitance C_{TEM} and mutual inductance M_{TEM} as

$$V_{\text{EC}}^{\text{RI}} = \omega C_{\text{TEM}} Z_{\text{out}} V_{\text{EMI}} \tag{6}$$

$$V_{\text{MC}}^{\text{RI}} = \omega M_{\text{TEM}} I_{\text{EMI}} \tag{7}$$

where V_{EMI} and I_{EMI} are the voltage and current of the EMI injected into the TEM cell, and Z_{out} is the detected terminal of the microstrip line. In most of actual EMC problems, the sensitive device is matched to the transmission line. Thus, Z_{out} is equal to Z_0.

Considering the termination effect from the load Z_{L}, the induced voltage of the microstrip line according to equivalent circuits of electric and magnetic field to a microstrip line couplings for radiated immunity in Fig. 3 is equal to

$$
\begin{aligned}
V_{\text{MS}}^{\text{RI}}(z) &= \frac{1}{2} \left(V_{\text{EC}}^{\text{RI}} \pm V_{\text{MC}}^{\text{RI}} \right) e^{j\beta z} + \frac{1}{2} \left(V_{\text{EC}}^{\text{RI}} \mp V_{\text{MC}}^{\text{RI}} \right) e^{-j\beta z} \\
&= \frac{1}{2} V_{\text{EC}}^{\text{RI}} \left(\left(e^{j\beta z} + \Gamma_0 e^{-j\beta z} \right) \right) \pm V_{\text{MC}}^{\text{RI}} \left(e^{j\beta z} + \Gamma_0 e^{-j\beta z} \right).
\end{aligned}
\tag{8}
$$

Figure 3. Equivalent circuits of electric and magnetic field to a microstrip line couplings for radiated immunity: (a) electric field coupling, (b) magnetic field coupling.

Since the length of the line is much less than the wavelength of induced voltage and current waves, the fluctuation of the induced voltage along the line can be normalized as

$$V_{\text{MS}}^{\text{RI}} = \frac{\displaystyle\int_0^l |V_{\text{MS}}^{\text{RI}}(z)| dz}{\displaystyle\int_0^l dz}. \tag{9}$$

2.3. Field-Line Coupling Model

Since 50-Ω systems are more common for electronic devices, the characteristic impedance Z_0 of investigated microstrip lines are set to $50\,\Omega$. For EMC analysis, the maximum induction is more

relevant. Combined with (5) and (9), electromagnetic field-microstrip transmission line coupling of a TEM cell can be consolidated as

$$V_{\text{induced}} = \frac{1}{2}\left(50\omega C_{\text{TEM}}V_{\text{EMI}}K_1 + \omega M_{\text{TEM}}\frac{V_{\text{EMI}}}{50}K_2\right) \tag{10}$$

where V_{induced} is the induced voltage at the output end of the line or the TEM cell; the coefficient K_1 and K_2 are equal to

$$K_1 = \frac{1}{l}\int_0^l |e^{j\beta z} + \Gamma_0 e^{-j\beta z}|dz \tag{11}$$

$$K_2 = \frac{1}{l}\int_0^l |e^{j\beta z} - \Gamma_0 e^{-j\beta z}|dz. \tag{12}$$

2.4. Coupling Impedance

C_{TEM} and M_{TEM} can be derived from two extreme terminations: shorted ($\Gamma_0 = -1$) and open ($\Gamma_0 = 1$):

$$C_{\text{TEM}} = \frac{K_2^{\text{S}}S_{21}^{\text{O}} - K_2^{\text{O}}S_{21}^{\text{S}}}{25\omega\left(K_2^{\text{S}}K_1^{\text{O}} - K_2^{\text{O}}K_1^{\text{S}}\right)} \tag{13}$$

$$M_{\text{TEM}} = 100\frac{K_1^{\text{O}}S_{21}^{\text{S}} - K_1^{\text{S}}S_{21}^{\text{O}}}{\omega\left(K_2^{\text{S}}K_1^{\text{O}} - K_2^{\text{O}}K_1^{\text{S}}\right)} \tag{14}$$

where S_{21} is the transfer coefficient equal to $V_{\text{induced}}/V_{\text{EMI}}$, and S_{21}^{O} stands for open termination and S_{21}^{S} for the shorted termination.

The characteristic impedance of a transmission line is specified in terms of its per-unit-length capacitance C and inductance L, $Z_{\text{c}} = \sqrt{L/C}$. Since the TEM cell is an approximate transmission line structure, we define a coupling impedance to describe the coupling characteristic of the TEM cell and the microstrip line

$$Z_{\text{coupling}} = \sqrt{\frac{M_{\text{TEM}}}{C_{\text{TEM}}}} = 50\sqrt{\frac{K_1^{\text{O}}S_{21}^{\text{S}} - K_1^{\text{S}}S_{21}^{\text{O}}}{K_2^{\text{S}}S_{21}^{\text{O}} - K_2^{\text{O}}S_{21}^{\text{S}}}}. \tag{15}$$

3. MEASUREMENT AND DISCUSSION

The couplings were measured by a vector network analyzer (VNA) Agilent N5224A (sketched in Fig. 4). The TEM cell is FCC-TEM-JM1 and operates up to 1.2 GHz. Microstrip lines with the same width of $w = 1\,\text{mm}$ were fabricated at the center of a square PCB ($\varepsilon_{\text{r}} = 4.2$) and ended by surface-mount SMA connectors. Two lengths of microstrip lines were chosen, 10 mm and 20 mm. All lines were designed to have a characteristic impedance of 50 Ω. One port of the VNA was connected to one end of the TEM cell and the other was connected to one SMA connector of a microstrip line. The other end of the TEM cell port was terminated with a 50 Ω load. The other SMA of microstrip lines was with an optional terminal load.
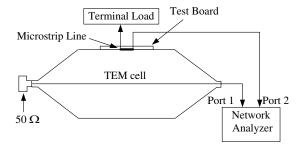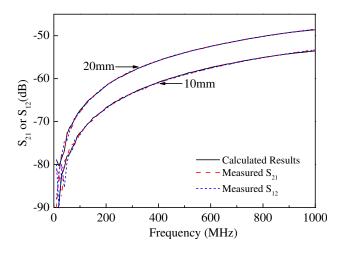

Figure 4. Setup for field-line coupling experiments of a TEM cell.

Measured and calculated S_{21} and S_{12} for matched lines are shown in Fig. 5. Measured results confirm the reciprocity of line-to-field and field-to-line couplings and have great agreements with calculated results for both lines. Then, coupling impedances Z_{coupling} of TEM cell and lines are plotted in Fig. 6.
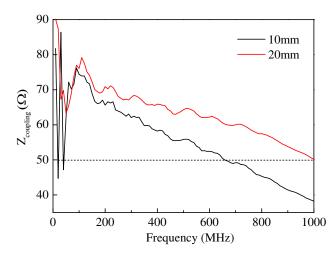

Figure 5. Measured and calculated S_{21} and S_{12} of microstrip lines ($l = 10\,\mathrm{mm}$ and $20\,\mathrm{mm}$, $w = 1\,\mathrm{mm}$) with matched termination ($50\,\Omega$).

Figure 6. The coupling impedance Z_{coupling} of TEM cell and microstrip lines ($l = 10\,\mathrm{mm}$ and $20\,\mathrm{mm}$, $w = 1\,\mathrm{mm}$).

Figure 7 shows the calculations of microstrip lines with arbitrary loads. It can be seen that the upper limitations of radiated emission and immunity of microstrip lines with arbitrary loads are determined by shorted or open termination. There is a cross point between S_{21} for shorted and open terminations: 650 MHz for the 10-mm line (see Fig. 7(a)) and 1 GHz for the 20-mm line (see Fig. 7(b)). From Fig. 6, it can be found that Z_{coupling} at the cross point for both lines are equal to $50\,\Omega$ and Z_{coupling} decreases with increasing frequency for both lines. The distance from the septum to the tested microstrip line inside the TEM cell is certain. Therefore, the fields inside the TEM cell change from induction fields to radiation fields with the operation frequency increasing. The near-zone induction fields for low frequencies are
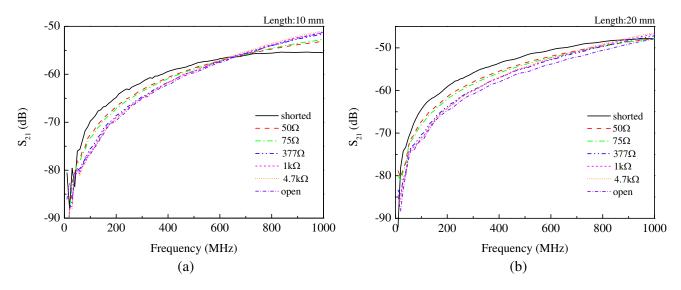

Figure 7. Calculations of microstrip lines with arbitrary loads: (a) $l = 10\,\mathrm{mm}$ and $w = 1\,\mathrm{mm}$, (b) $l = 20\,\mathrm{mm}$ and $w = 1\,\mathrm{mm}$.

quasi-static fields and the field-line coupling for these frequencies is mostly attributed to electric field or magnetic field. Then, the coupling impedance is not quite proper to describe the coupling behavior, as seen in Fig. 6 when the frequency is below 100 MHz.

Take the 10-mm line for example (Fig. 7(a)). When frequency is below the cross point, S_{21} of lines with shorted termination is the upper limitation which means that magnetic field coupling dominates the coupling. On the contrary, when frequency is beyond the cross point, S_{21} of lines with open termination is the upper limitation which means that electric field coupling dominates the coupling. Thus, the coupling impedance Z_{coupling} can be used to evaluate the domination of electric and magnetic fields in the field-line coupling. Magnetic field coupling is predominant when Z_{coupling} is over $50\,\Omega$, while electric field coupling is predominant when Zcoupling is below $50\,\Omega$. From Fig. 6, it can be found that the field inside the TEM cell measurement is radiated near field and the magnetic field mainly dominates.

4. CONCLUSION

In this paper, we present an analytic model to compliant both field-to-line and line-to-field couplings in a TEM cell. This model is available for line-length less than $30\,\mathrm{mm}$ (1/10 wavelength of $1\,\mathrm{GHz}$). Since the characteristic impedance of a TEM cell is equal to 50, the coupling impedance over or below $50\,\Omega$ can be used to determine the domination between electric field and magnetic field of the field-line coupling. This approach can be extended to other radiated emission and immunity measurements. For example, the coupling impedance equal to $377\,\Omega$ is the demarcation of the domination between electric and magnetic couplings for open-area test site or EMC anechoic chamber measurements.

ACKNOWLEDGMENT

REFERENCES

1. Kasturi, V., S. Deng, T. Hubing, et al., "Quantifying electric and magnetic field coupling from integrated circuits with TEM cell measurements," *Proc. IEEE Int. Symp. Electromagnetic Compatibility*, Vol. 2, 422–425, 2006.

2. Deng, S., T. Hubing, and D. Beetner, "Characterizing the electric field coupling from IC heatsink structures to external cables using TEM cell measurements," *IEEE Trans. on Electromagnetic Compatibility*, Vol. 49, No. 4, 785–791, 2007.

3. Deng, S., T. Hubing, and D. Beetner, "Using TEM cell measurements to estimate the maximum radiation from PCBs with cables due to magnetic field coupling," *IEEE Trans. on Electromagnetic Compatibility*, Vol. 50, No. 2, 419–423, 2008.

4. Shi, C., W. Fang, C. Chai, et al., "Using termination effect to characterize electric and magnetic field coupling between TEM cell and microstrip line," *IEEE Trans. on Electromagnetic Compatibility*, Vol. 57, No. 6, 1338–1344, 2015.

5. Vanhee, F., J. Catrysse, R. Gillon, et al. "Scalable equivalent circuit modelling of the EM field coupling to microstrips in the TEM cell," *IEEE International Zurich Symposium on Electromagnetic Compatibility*, 1–6, 2009.

6. Mandic, T., F. Vanhee, R. Gillon, et al. "Equivalent circuit model of the TEM cell electric and magnetic field coupling to microstrip lines," *IEEE International Conference on Electronics, Circuits, and Systems*, 247–250, 2009.

7. Mandic, T., R. Gillon, B. Nauwelaers, et al., "Characterizing the TEM cell electric and magnetic field coupling to PCB transmission lines," *IEEE Trans. on Electromagnetic Compatibility*, Vol. 54, No. 5, 976–985, 2012.

8. Op t Land, S., R. Perdriau, M. Ramdani, et al., "Simple, Taylor-based worst-case model for field-to-line coupling," *Progress In Electromagnetics Research*, Vol. 140, 297–311, 2013.

9. Op t Land, S., M. Ramdani, R. Perdriau, et al., "Using a modified Taylor cell to validate simulation and measurement of field-to-shorted-trace coupling," *IEEE Trans. on Electromagnetic Compatibility*, Vol. 56, No. 4, 864–870, 2014.

10. Mandic, T., B. Pejcinovic, and A. Baric, "Comparison of simulation and measurement of time-domain field-to-line coupling in TEM cell," *Proc. Int. Symp. on Electromagnetic Compatibility (EMC Europe)* 681–685, 2014.

11. Shi, C., C. Chai, Y. Yang, et al., "Estimating termination effect on electric and magnetic field-to-line coupling for radiated immunity tests using a TEM cell," *Progress In Electromagnetics Research Letters*, Vol. 60, 39–44, 2016.

12. "Integrated circuits — Measurement of electromagnetic emissions, 150 kHz to 1 GHz - Part 2: Measurement of radiated emissions, TEM-cell method and wideband TEM cell method (150 kHz to 8 GHz)," *IEC 61967-2*, 2001.

13. "Integrated circuits — Measurement of electromagnetic innunity, 150 kHz to 1 GHz - Part 2: Measurement of radiated immunity-TEM cell method," *IEC 62132-2*, 2003.

14. Ludwig, R. and G. Bogdanov, *RF Circuit Design Theory and Applications*, 2nd Edition, Publishing House of Electronics Industry, Beijing, 2010.